



Seismic moments of earthquakes in the Baikal rift zone as indicators of recent geodynamic processes

Anatoly V. Klyuchevskii*

*Institute of the Earth Crust, Siberian Branch of the Russian Academy of Sciences,
Ul. Lermontova 128, Irkutsk, 664033 Russia*

Received 28 June 2002; received in revised form 19 December 2003; accepted 7 January 2004

Abstract

The investigation of spatio-temporal variations of seismic moments of earthquakes in the Baikal region shows three considerable episodes of change of the state of stress and strain of the Earth's crust between 1968 and 1994. The changes in the state of stress and strain are due to the variations of vertical component of S_V -stresses. They testify to the fact that rifting can have a pronounced effect on recent geodynamic processes in the Baikal region.

© 2004 Elsevier Ltd. All rights reserved.

1. Introduction

The Baikal seismic zone (BSZ) is located in the southeastern part of the Russian Federation north of Mongolia between 48° – 60° N latitude and 96° – 122° E longitude. Up to 200 earthquakes with the Love wave magnitude $M_{LH} \geq 3.0$ occurred there within the last 260 years, 70 of those recorded by regional seismic stations. The Baikal rift zone (BRZ), extending from Northern Mongolia along Lake Baikal to Southern Yakutia as a system of rift basins, is the most seismically hazardous in the BSZ. The epicentral map of earthquakes with $M_{LH} \geq 3.0$ recorded by the regional seismograph network from 1964 to 1997 gives an indication of the high seismic potential of the BRZ (Fig. 1). The map shows that the seismic areas take the form of bands trending NE along the rift structures (Golenetsky, 1990; Solonenko et al., 1996). The study of the spatio-temporal distribution of the earthquakes reveals the alternation of low and high seismicity and the

* Corresponding author. Tel.: +7-3952-42-74-62.

E-mail address: akluchev@crust.irk.ru

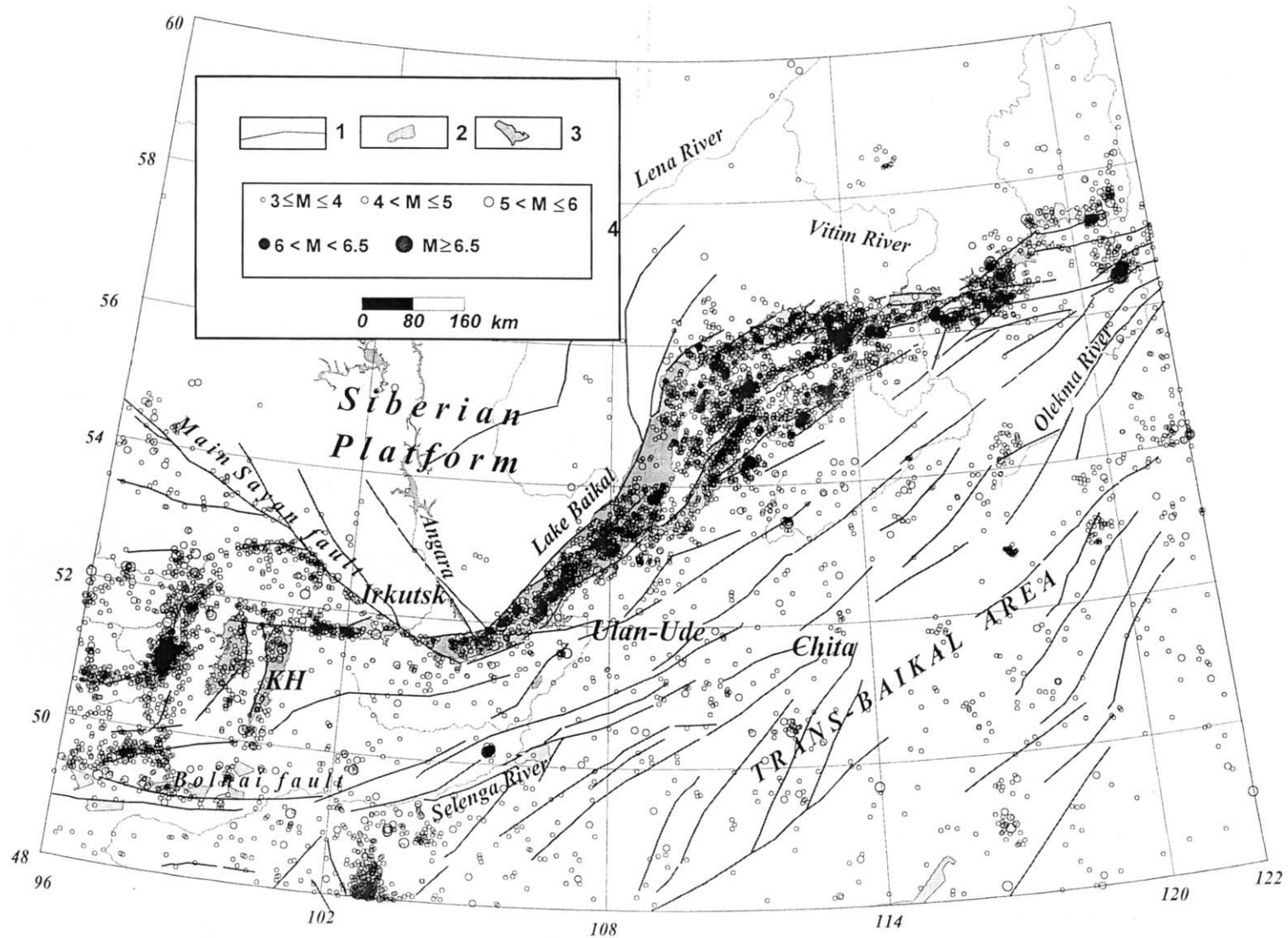


Fig. 1. Epicenters of $M_{LH}=3 \div 7$ earthquakes in the Baikal seismic zone for 1964–1997. 1—Faults active in Cenozoic; 2—basins; 3—lakes; 4—earthquake epicenters; KH—Lake Khubsugul.

fact that the aftershocks or earthquake swarms often produce local groups of high-concentration earthquake epicenters. A scattered seismicity prevails beyond the rift zone.

Study of the state of stress and strain of the Earth's crust in the region shows the dominance of tensile stresses oriented across the strike of basic morphostructures on considerable parts of the BRZ (Zoback, 1992a). However, the extensional regime does not dominate on the flanks of the rift zone and beyond it (Petit et al., 1996; Solonenko et al., 1997). It has been recently found that the stress field in the rift zone can undergo significant spatio-temporal variations that result in the change of focal mechanisms and seismic moments of the earthquakes (Dyadkov et al., 2000; Klyuchevskii, 2000). The central part of the rift zone is characterized by an abrupt change of thickness of the Earth's crust and by a large number of faults. The Earth's crust in the central part of the region is deformed to a greater degree than on the flanks and margins, and the largest deformation of the medium is found within the South Baikal basin (Klyuchevskii and Demyanovich, 2002a). This area is probably the earliest element of the Baikal rift system (Logatchev, 1993).

Seismic moments of earthquakes are usually characterized by correlation equations with energy class K or magnitude M_{LH} . Magnitudes M_{LH} are generally converted from the Russian energy class by the formula $K = 1.8M_{LH} + 4$ (Rautian, 1964). Derived in such a way the whole set of shocks may yield sampling data sufficient for statistical processing and computing of the coefficients in the regression equations. The study of seismic moments of earthquakes in a number of areas of the BSZ and Mongolia shows that the coefficients in the regression equations may vary with regard to place, time and kind of seismic process (Klyuchevskii, 1998, 2000). The variations of coefficients reflect the variations in seismic moments of earthquakes and carry information on variations in the state of stress and strain of the medium.

The present paper considers spatio-temporal variations of seismic moments of small and moderate earthquakes in the BRZ. The results help to understand the physical processes that generated the observed variations of seismic moments in the spatio-temporal continuum.

2. Data and method of investigation

The data are taken from the 1968 to 1994 “Seismic reports for the Baikal region” that contain the basic items of information on earthquakes in the BSZ. The amplitudes and periods of the maximum displacements in S -waves for about 70,000 earthquakes of magnitude $2.0 \leq M_{LH} \leq 5.5$, recorded throughout the BSZ from 1968 to 1994, were used as the initial data. The earthquakes of $M_{LH} \geq 2.5$ in the region have been recorded without omission since the middle 1960s (Golenetsky, 1990). Due to the fact that some of the shocks of $M_{LH} = 2$ might have been missed, the correlation equations are derived for sets of earthquakes of $M_{LH} \geq 2$ and $M_{LH} \geq 2.5$.

The source parameters of small shocks are primarily determined through comparison between the Fourier amplitude spectra, computed from the instrumental records, and theoretical models of the earthquake source. J. Brune's formulas for the dynamic crack model (1970) are used in the present work. Seismic moments of the earthquakes are calculated as

$$M_0 = 4\pi\rho R\beta^3 F_0 / \Psi_{\theta\varphi}, \quad (1)$$

where M_0 is the seismic moment [dyn cm], $\rho = 2.7 \text{ gr/cm}^3$ is the density, $\beta = 3.58 \text{ km/s}$ is the shear wave velocity, R is the hypocentral distance [km], and $\Psi\theta\varphi = 0.6$ is a parameter that takes into account the radiation pattern.

The maximum amplitude and the period of an analogue record of seismic ground motion are converted into the level of spectral density $F\hat{i}$, from which one obtains the corner frequency f_o . The procedure of conversion was developed on the basis of more than 200 seismograms, spectrograms and Fourier amplitude spectra of the records of earthquakes in the BSZ with magnitudes $M_{\text{LH}} = 1.0 \div 5.0$. The earthquake spectrograms were obtained through decomposition of magnetic records by a block of eleven filters of spectral analyzer. The following formula relates the maximum amplitude recorded by each filter to the same-period value of the Fourier amplitude spectrum

$$A \pm 0.001 = (0.042 \pm 0.001)T, \quad (2)$$

where $A = F/Aa$, F is the level of amplitude spectrum in period T [mm s], and Aa is the maximum amplitude recorded by corresponding filter of spectral analyzer [μm]. The equation of regression between the frequency of maximum on the record and that on the spectrogram takes the form

$$f_1 \pm 0.10 = (0.95 \pm 0.01) f_2 + (0.08 \pm 0.07), \quad (3)$$

where f_1 is the frequency of the maximum amplitude on a seismogram [Hz], and f_2 is the frequency of the filter with the maximum recording level [Hz]. As the frequency of filtering is kept constant for each filter at the same speed of magnetic tape, the analyzer may be considered as reproducing the frequency of the maximum amplitude without distortions. The correlation between the maximum amplitude on the record and the maximum level of the spectrogram depends upon the period T_1 of the maximum amplitude as

$$B \pm 0.04 = (1.97 \pm 0.07) T_1 + (1.63 \pm 0.03), \quad (4)$$

where $B = A_1/A_2$, A_1 being the maximum amplitude on the seismogram [μm], and A_2 the maximum level of spectrogram [μm]. Eq. (2) allows determination of the level and shape of the Fourier smoothed amplitude spectrum. Eqs. (3) and (4) allow the calculation of the level and frequency of the spectrogram maximum. In total, these equations make it possible to calculate the maximum level of the Fourier amplitude spectrum and the upper frequency of the maximum level from the values of amplitude and period of maximum displacement on the seismogram.

The determination of “coordinates” of the corner point of the Fourier amplitude spectrum from the analog record consists of the conversion of the maximum amplitude into the level of spectral density F_o , and the oscillation frequency into the frequency of the corner point f_o . In J. Brune’s theoretical model the level of spectral density remains constant on frequencies lower than the corner point and decreases under the ω^{-2} law for higher frequencies. For near earthquakes, the maximum amplitude of an analog record is many times higher than the remaining amplitudes, and will correspond to the maximum level of the amplitude spectrum. The frequency of the maximum amplitude of the record will correspond to that of the corner point, as otherwise the analog record would have had at least one high-frequency oscillation with the level of amplitude spectrum not lower than that of the maximum oscillation amplitude. For distant earthquakes, the maximum amplitude is higher than that of nearby oscillations. The corner point in this case is determined by a set of amplitudes and periods that provide the maximum level of spectral density.

Comparison among results obtained by using Fourier amplitude spectra shows that the maximum difference between single determinations of seismic moments may reach 60% and the maximum difference between the average radii of dislocation may reach 50%. The shape of histograms corresponds to a Gaussian distribution. The procedure has the advantage that dynamic parameters are determined consistently without a subjective evaluation of the level of amplitude spectrum and the corner frequency of each earthquake. Such simplified formalized evaluation of dynamic parameters allows using a huge quantity of seismological information accumulated in the Baikal region by seismic stations of galvanometric registration.

An assessment of uncertainty in the determination of corner frequency of Fourier amplitude spectra has been made for seismic shocks of magnitudes from 1.8 to 4.9 (Hough and Dreger, 1995). The determination of corner frequency becomes more accurate with increasing magnitude. A comparison between simulated and real spectra shows that the scatter of corner frequency might be about an octave. Energy classes of earthquakes of the Baikal region, calculated from the sum of maximum amplitudes of *P*- and *S*-waves, have uncertainties up to 0.5 class unit. Depending on the relationship between logarithm of seismic moment and energy class of earthquakes, the uncertainty introduced into the moment value by oscillations in amplitude may be 0.25–0.3 units of the moment logarithm. During the change of corner frequency by an octave, the variations of seismic moment reach 0.1–0.2 units of logarithm moment. The uncertainties of determination of seismic moment by the present procedure may therefore be 0.3–0.5 units of the logarithm of seismic moment. In the present work, an efficient seismic quality factor of the medium does not depend on the frequency and has a large value, and the coefficient of geometric spreading is $n = 1$. Of consideration are seismic signal doubled on a free surface and the use of one horizontal component of the record of the maximum amplitude of displacement.

To compare seismic moments of the earthquakes determined by international agencies with those determined by the present procedure, the data on the large shocks that occurred within BSZ from 1968 to 1997 and whose moments have been determined were downloaded from Internet (Bulletin of the International Seismological Center, BISC). Eight coinciding events were found as

Table 1

Basic data on the large BSZ earthquakes with the seismic moments determined in parallel with the international agencies

No.	Date	Time	Coordinates		<i>mb</i>	M_0 (CMT)	M_0	<i>S</i> ,%
			φ , degree	λ , degree				
1	1987.07.07	17-07-28.5	56.55	121.10	5.0	$9.0 \cdot 10^{23}$	$8.9 \cdot 10^{23}$	1
2	1989.10.25	20-29-01.9	57.45	118.84	5.5	$1.6 \cdot 10^{24}$	$1.3 \cdot 10^{24}$	19
3	1990.10.26	18-17-35.7	55.95	110.25	5.1	$7.9 \cdot 10^{23}$	$1.3 \cdot 10^{24}$	–65
4	1991.09.12	00-33-30.8	54.82	111.15	5.1	$6.4 \cdot 10^{23}$	$7.9 \cdot 10^{23}$	–23
5	1992.02.14	08-18-26.0	53.83	109.00	5.4	$1.3 \cdot 10^{24}$	$1.5 \cdot 10^{24}$	–15
6	1994.04.26	18-59-27.8	56.72	118.04	5.5	$1.5 \cdot 10^{24}$	$1.0 \cdot 10^{24}$	33
7	1995.06.29	23-02-27.2	51.71	102.70	5.5	$5.2 \cdot 10^{24}$	$8.7 \cdot 10^{23}$	83
8	1995.11.13	08-43-15.4	56.13	114.55	5.9	$5.7 \cdot 10^{24}$	$8.9 \cdot 10^{24}$	–56

Date, time and coordinates are taken from the “Earthquake Catalog for the Baikal region”; *mb* and M_0 (CMT) [dyn cm]—the magnitude and the seismic moment of the earthquake are taken from the BISC; M_0 [dyn cm] is the seismic moment determined in this study; *S*,% is a relative error, percentage.

a whole, with the basic parameters given in Table 1. Seismic moments M_o (CMT) in Table 1 were taken for comparison as the most frequently met in BISC. Seismic moments of the largest earthquakes in BSZ are sometimes determined by several agencies. Thus, the seismic moment of the South-Yakutian earthquake (1989.04.20, 22-59-54.8, $\varphi = 57.17^\circ$ N latitude, $\lambda = 122.31^\circ$ E longitude, $K = 16.5$, $mb = 6.2$) is $M_o = 2.9 \cdot 10^{18}$ [N-m] from the USGS data, $M_o = 5.0 \cdot 10^{18}$ [N-m] from the GEOSCOPE data, and M_o (CMT) = $3.1 \cdot 10^{18}$ [N-m] (Newton-meter). The uncertainties of the moment value are 70% that almost coincides with the maximum uncertainty S in the table. Unfortunately, the dynamic parameters of such large shocks can not be determined because of the lack of the indispensable data in “Seismic reports for the Baikal region”.

3. Results

Fig. 2 shows a map of isolines of logarithm of the total seismic moment of earthquakes in the Baikal region. It is obtained by summation of seismic moments of the earthquakes of magnitude $M_{LH} \geq 4$ in $1.0^\circ \times 1.5^\circ$ sites and drawn from $\lg M_o \geq 22$. The isolines appear as separate figures, that vary in size and shape and are extending from the southwest to the northeast. Local maximums exceeding $\lg M_o > 24$ in the southwestern and northeastern flanks and the central part of the BSZ are distinguished. Note that the map reflects only approximately the distribution of the total seismic moment throughout the BSZ, as it does not consider some of the large and any of small (up to $M_{LH} = 3.5$) shocks.

The map can be divided into three regions. The first region is located in the southwestern flank of the BSZ between $\varphi = 48^\circ - 53^\circ$ N latitude and $\lambda = 96^\circ - 104^\circ$ E longitude. The second region identified in the central part of the BSZ is limited to $\varphi = 51^\circ - 54^\circ$ N latitude and $\lambda = 104^\circ - 113^\circ$ E longitude. The third region ($\varphi = 54^\circ - 58^\circ$ N latitude, $\lambda = 109^\circ - 122^\circ$ E longitude) is in the northeastern flank of the BSZ. For a detailed investigation of spatial variations of the seismic moments, each of these regions was divided along the respective $\lambda = 100^\circ$ E; $\lambda = 108^\circ$ E and $\lambda = 116^\circ$ E longitude into two sites approximately equal in area. For the sake of convenience we number these regions sequentially as 1, 2 and 3 and the sites as 1–6 from the southwest to the northeast.

We use c -coefficients in the correlation equations for logarithm of the moment and energy class of the shocks to investigate spatial and temporal variations of the seismic moments

$$\lg M_o \pm S = (A \pm Sa) + (c \pm Sc)K, \quad (5)$$

where A and c are the coefficients, and S , Sa and Sc are the mean square deviations. The equations are derived for one-, two- and three-year sets of the earthquakes of $M_{LH} \geq 2$ and $M_{LH} \geq 2.5$ that occurred within the BSZ, three regions and six sites. A comparative analysis of the results indicates that the curves of temporal variations of c -coefficient coincide at 10% level of significance (Fig. 3), and increasing duration of a set tends to smooth the curves. The curves obtained for one-year sets of earthquakes of $M_{LH} \geq 2$ provide an optimum example of the spatio-temporal variations of c -coefficients. The minimum number of shocks in a set is 64.

Fig. 4 illustrates the curves of the variation of c -coefficient throughout the BSZ and three regions. The curves of c -coefficients correlate well with each other in all the areas. The superposing error bands, however, complicate the analysis. Therefore, they are only shown in Figs. 5

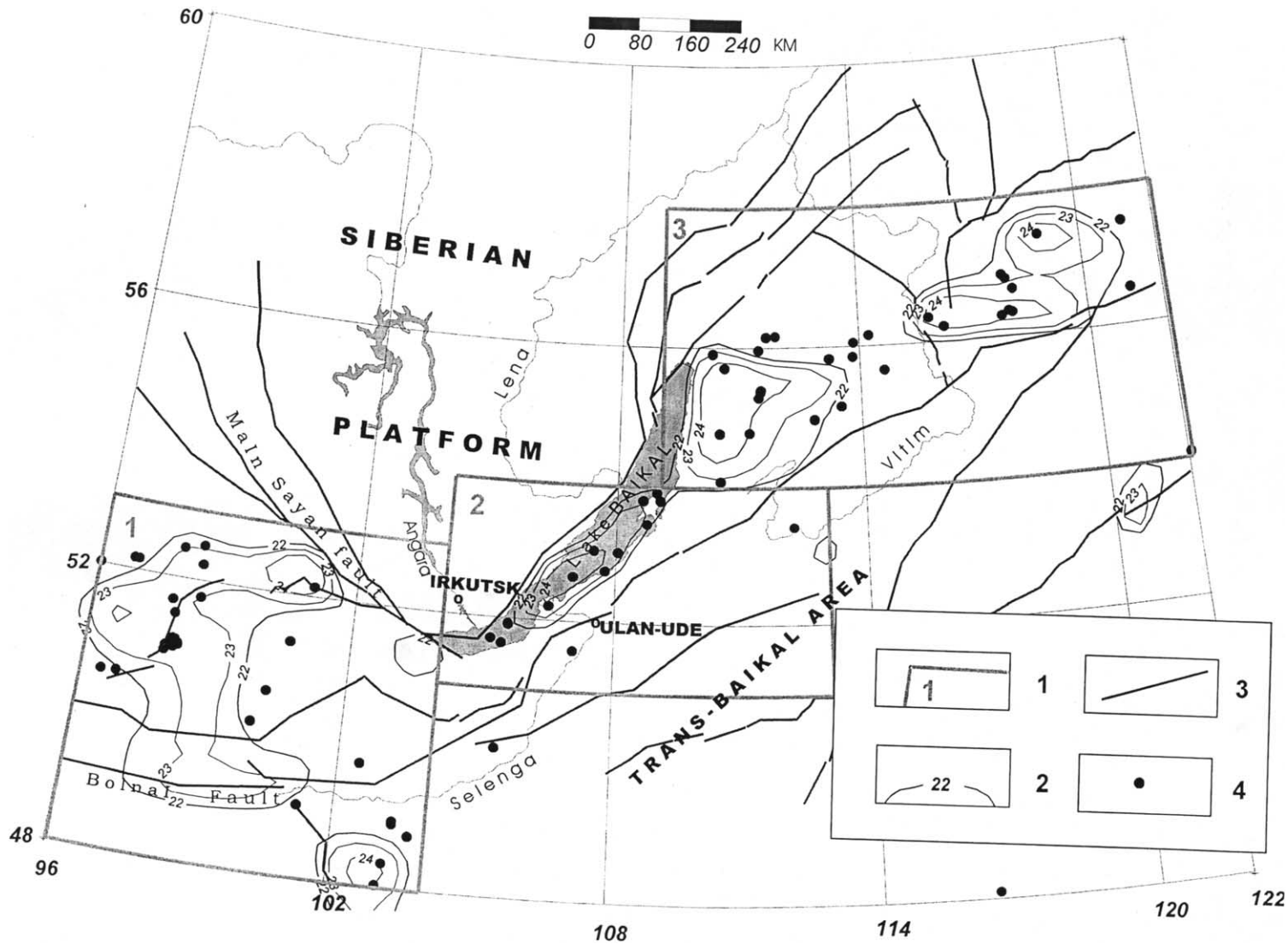


Fig. 2. Isolines of the logarithm of the total seismic moment. 1—Borders of the investigated sub-regions; 2—isolines for the logarithm of the total seismic moment; 3—major faults; 4—earthquake epicenters $M_{LH} \geq 5$.

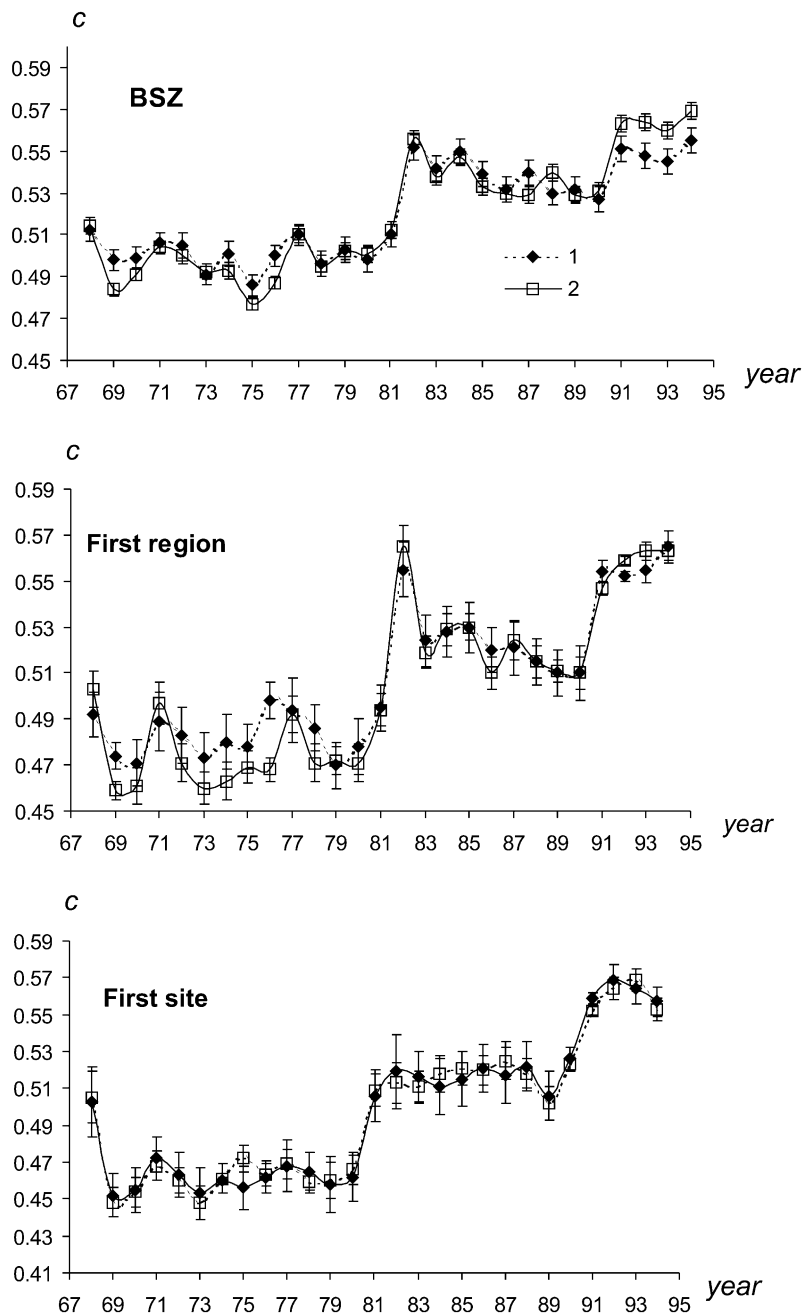


Fig. 3. Variations of C-coefficients in the BSZ, in the first region and in the first site. 1— $M_{LH} \geq 2.5$; 2— $M_{LH} \geq 2.0$.

and 6 for the territory of primary interest. The “special” temporal points are provided with the correlation equations allowing one to evaluate the significance of the coefficients and equations as a whole. The most important feature of the curves in Fig. 4 is the *c*-coefficient rising sharply in the late 1970s to early 1980s. The first change of *c* is noted in 1979 within the second region. The correlation equations for the seismic moment and energy class of earthquakes in the BSZ and in the second region for 1979 are derived as

$$\begin{aligned} \lg M_0 \pm 0.48 &= (17.12 \pm 0.04) + (0.502 \pm 0.004)K, \\ \rho &= 0.954 \pm 0.003, \quad F = 11.0, \quad n = 1131 \end{aligned} \tag{6}$$

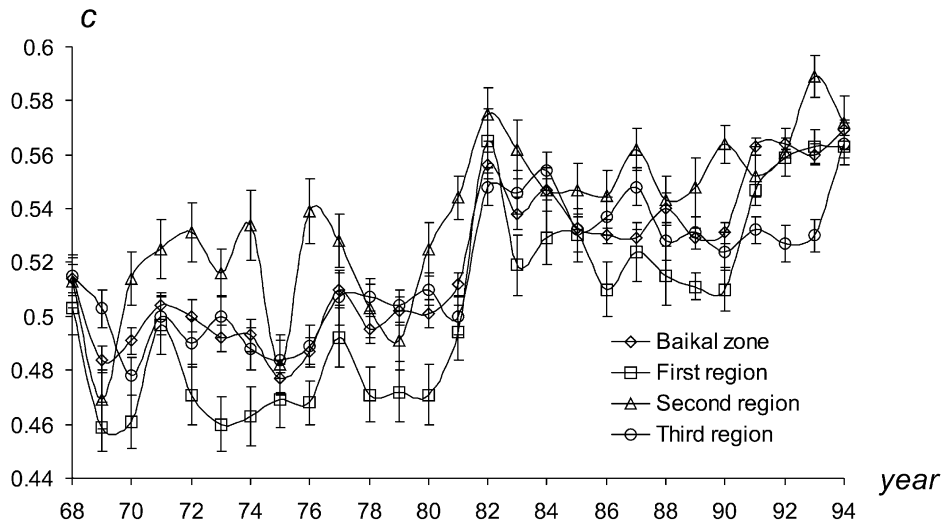


Fig. 4. Variations of *C*-coefficients in the BSZ and in the first—third regions.

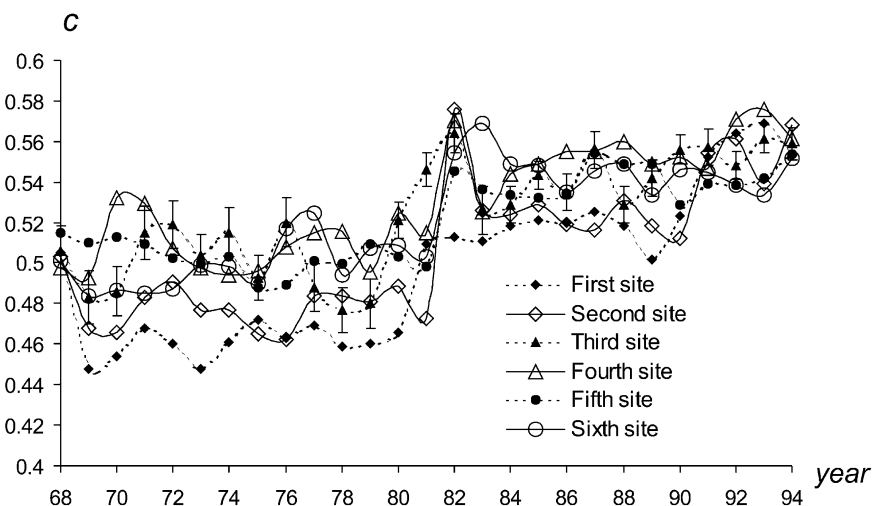


Fig. 5. Variations of *C*-coefficients in the first—sixth sites.

$$\lg M_0 \pm 0.43 = (17.22 \pm 0.11) + (0.49 \pm 0.01)K, \quad \rho = 0.94 \pm 0.01, \quad F = 8.23, \quad n = 207; \quad (7)$$

where ρ is the correlation coefficient, F is the Fisher criterion, and n is the number of shocks.

To localize this phenomenon, further investigation is done from the data on the shocks occurred within six sites (Fig. 5). Fig. 5 demonstrates that the c -coefficient is increasing in different ways in the second, fourth, fifth and sixth sites, and in the first and third sites. In the first case (sites 2, 4, 5 and 6) a sharp increase of c -coefficient is only occurring in 1981. In the second case (sites 1 and 3) c -coefficient starts increasing in 1979 in the territory of the third site, and in 1980 in that of the first site. The maximum c -value is observed in 1982 in the first-fifth sites and in 1983 in the sixth site. The correlation equation for the seismic moment and energy class of earthquakes in the third site for 1979 takes the form

$$\lg M_0 \pm 0.43 = (17.29 \pm 0.10) + (0.48 \pm 0.01)K, \quad \rho = 0.94 \pm 0.01, \quad F = 8.70, \quad n = 194. \quad (8)$$

The analysis of the plots of the correlation between the seismic moment and energy class of 1978–1984 earthquakes within six sites indicates that the growing seismic moments cause the sharply increasing c -coefficients.

Spatio-temporal localization of the growing seismic moments is continued for earthquakes of the third site divided along the latitude into three zones and along the longitude into four sectors that are one degree in width. The average number of earthquakes that occurred in these bands within a year is more than 30. Fig. 6 shows the curves of c -coefficient varying throughout the third site and four sectors. With regard to the time period of interest, c -coefficient is the minimum in 1978–1979, increasing then and reaching its maximum in 1981–1982. The extremes of 1978 and 1981 correspond to the curve of c -variations in the third sector. The correlation equation for the seismic moment and energy class of earthquakes occurred in this sector in 1978 is of the form

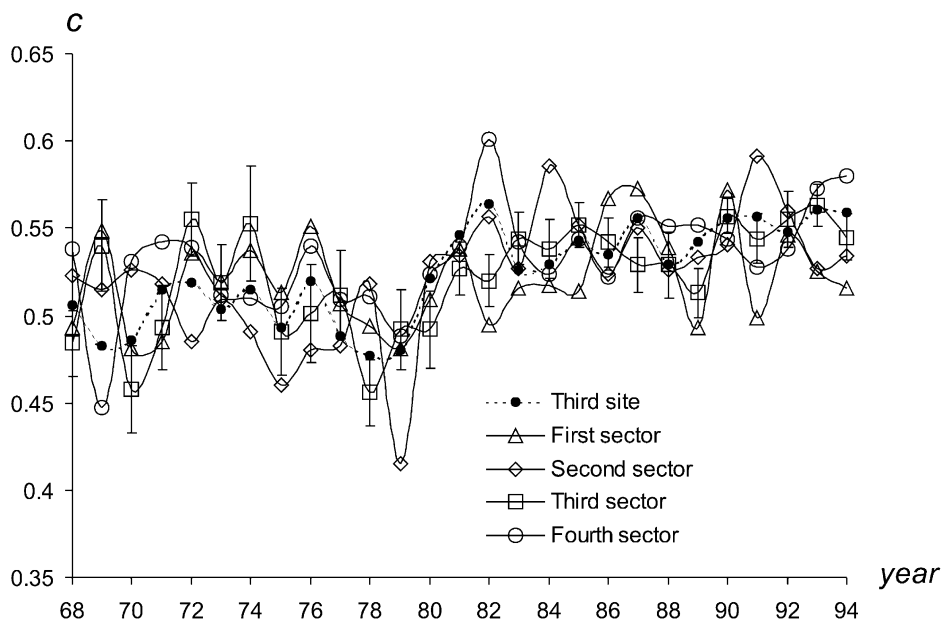


Fig. 6. Variations of C -coefficients in the third site and in the first—fourth sectors.

$$\lg M_0 \pm 0.43 = (17.49 \pm 0.15) + (0.46 \pm 0.02)K, \quad \rho = 0.95 \pm 0.01, \quad F = 9.71, \quad n = 61; \quad (9)$$

Note that Eqs. (6)–(9) describe the initial data at the level of significance not lower than 2.5%.

The data on the seismic events of $M_{LH} = 2 \div 4.5$ in the Baikal region were used in calculations of the average annual seismic moments of the earthquakes. Fig. 7 displays curves of the variations of the average annual seismic moments of the shocks in the BSZ showing a tendency of the seismic moments to increase with time for the investigated period. This tendency is small for the shocks of $M_{LH} = 2 \div 3$, but the correlation coefficient is $\rho \approx 0.6\text{--}0.7$ for larger earthquakes. The increase of levels of the average seismic moments of the shocks of each magnitude was the most intensive in the time period of interest. The seismic moments of the earthquakes of $M_{LH} = 2 \div 2.5$ began to grow in 1980. This growth was 20% within a year at 2% standard deviation of the average. The average seismic moments of the shocks of $M_{LH} = 3 \div 4$ increased in 1981, and those of earthquakes of $M_{LH} = 4.5$ increased in 1982. In all cases the increments of the seismic moments are far in excess of the standard deviation.

It is known that dynamic parameters of tectonic earthquake sources depend on faulting. In particular, a normal fault has less seismic moment than a strike-slip at an equal magnitude (Kopnichev and Spilker, 1980). The increasing seismic moments of the earthquakes in the BSZ in late 1970s to early 1980s can be attributed to the normal-fault shocks relatively decreasing in number in annual sets of the earthquakes. This might have resulted from the switch of the principal and intermediate stress axes, systematically noted in the earthquake sources in the Baikal rift. In this connection it is appropriate to consider the variations of seismic moments of the earthquakes for the whole time period. Fig. 4 shows a rather sharp decrease in c -coefficient for all the areas in the late 1960s. A decrease in the average annual seismic moments of the shocks is shown in Fig. 7 for the same time period. As the process began prior to 1968, it is impossible to

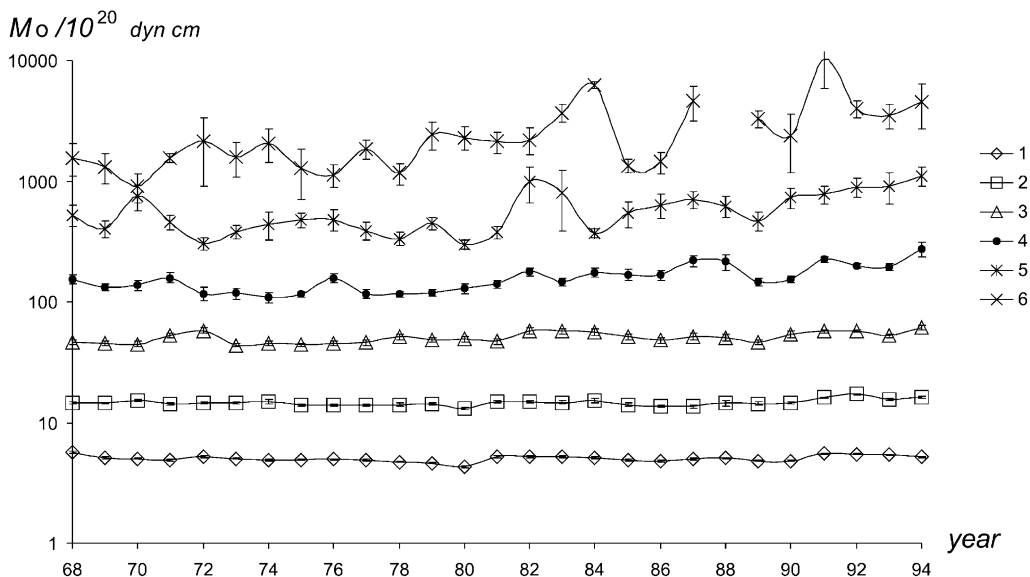


Fig. 7. Average annual seismic moments of earthquakes in the Baikal region. 1–6—Shocks of different magnitude $M_{LH} = 2.0, 2.5, 3.0, \dots, 4.5$.

analyze it now because of the lack of data. The coefficient was fixed at the average level for about the next 10 years (Fig. 4). A sharp increase in c -coefficient in the late 1970s to early 1980s can be interpreted as a relatively decreasing number of normal-fault shocks and as decreasing activity of rifting. In the following 10 years it was fixed at the average level again for the earthquakes in each area. The next increase in c -coefficient is observed in the late 1980s to early 1990s, first in the southwestern, then in the central and, finally, in the northeastern areas. The average annual seismic moments of the earthquakes also increase at that time (Fig. 7). It is indicative of the annual sets growing in a number of shocks that were not normal faults. The reverse-fault shocks sharply increased in number in the Baikal region at that time (Dyadkov et al., 2000).

4. Discussion and conclusion

Two hypotheses have been proposed to explain the occurrence of intraplate seismicity (Zoback, 1992b). The first is the reactivation of preexisting faults in a uniformly oriented regional stress field with the near-horizontal and near-vertical trending principal planes. As the plate-driving forces probably are the source of this relatively uniform broad-scale regional stress field, the latter should be time-invariant in the intraplate setting. The second hypothesis is local stress perturbation. In this case the sense or orientation of the slip recorded for the intraplate events is incompatible with the regional stress field. Instead, it is closely related to local stress anomalies such as lateral variations in the crustal structure, lithologic or strength contrasts, and stress concentrations along the edges of structures and bodies. Noteworthy is the fact that the stress field in this case should be also time-invariant for the reference time periods.

Spatio-temporal variations of the seismic moments of the earthquakes in the late 1970s to early 1980s, and late 1980s to early 1990s can be explained in the framework of the Baikal rifting model. This model combines the influence of asthenospheric upwelling (Logatchev and Zorin, 1987; Gao et al., 1994) and intense deformation of the lithospheric plates during the Indo-Asian collision (Molnar and Tapponnier, 1975). The phenomenon that caused spatio-temporal variations of the seismic moments of the earthquakes in the Baikal region in the late 1970s to early 1980s had the following properties. (1) It exerted its influence throughout the territory of the Baikal region. (2) Started in the third site and the process manifested itself in the first one approximately in a year. (3) One more year after it began acting in the rest of four sites, which are away from each other. (4) This action continued for a year and was followed by the decrease in the first-fifth sites and the maximum of influence in the sixth site.

The South Baikal basin, with the uplift of a mantle diapir, is located within the third site (Logatchev, 1993). The first changes of the seismic moments of the earthquakes occurred in the third sector of this site. The localization could be more detailed considering that the northern part of the sector is situated on the territory of aseismic Siberian platform, and about 90% of the shocks occurred within the area of $\varphi = 52\text{--}53^\circ$ N latitude and $\lambda = 106\text{--}107^\circ$ E longitude. This area coincides with the zone of maximum deformation of the Earth's crust in the BRZ (Klyuchevskii and Demyanovich, 2002a). So, the variations of c -coefficient were for the first time observed in 1978 in the most highly deformed locality of the suture zone separating the Siberian platform from the young Sayan-Baikal folded area. As far as we know (Logatchev and Zorin, 1992), the thickness of the lithosphere peaks (200 km) beneath the Siberian platform. It is reduced to 40–50

km beneath the southern folded framing of the platform superposed by the Late Cenozoic Baikal rift zone. Beneath the lithosphere there is anomalous mantle. The seismic and magnetotelluric data show an asymmetry of the asthenospheric high—subvertical limits from the Siberian platform and its gradual southeastward deepening. Relying on this data, the lower part of the suture can be simulated as subvertical separation between solid and plastic substance with temperature close to melting point.

The process of inversion of the principal and intermediate stress axes started in the most highly deformed area of the suture zone. The shocks that are not normal faults relatively increase in number, having their seismic moments higher than the normal-fault shocks of the same magnitude range. The process of inversion develops with time and results in the change of the state of stress and strain of the Earth's crust at the site, region and BRZ and, finally, in the change of focal mechanisms and increase of the seismic moments of the earthquakes in these regions. The change of the state of stress and strain of the Earth's crust should be primarily recorded by small shocks. It is illustrated by the curves (Figs. 4 and 5) showing the reduction of c -values that is due to the increase of the seismic moments of small shocks. The c -coefficients are reduced before a sharp increase in their values responsible for the increase of the seismic moments of rather large earthquakes in the third region and in the second and fourth–sixth sites. Such reduction of c -coefficient is not observed in the first and second regions and in first and third sites, as these areas are sources of transformation of the state of stress and strain of the medium.

The local character of the phenomenon of the late 1970s to early 1980s and its effect in decreasing the principal compressional stress S_V are confirmed by dynamic variations of the curves (Figs. 4 and 5). These variations are caused by small, moderate and large earthquake effects while the stress axes invert in small volumes of the Earth's crust. Within the framework of this investigation, one can only note that such synergetic self-organizing phenomena in the Baikal region arise from stress transitions in the most deformed volumes of the Earth's crust, producing a sharp increase in the number of earthquake swarms, i.e. small shocks. The self-organizing processes are mostly of a rifting nature and consist of cycles of different tempo, beginning as local structures-attractors (Klyuchevskii, 2003). Quite different, smooth variations of the curves in the late 1980s to early 1990s correspond to a wide front of disturbance, at a gradually extending area of influence without change of earthquake swarm activity. An increase in horizontal compression from the southwest to the northeast corresponds in the Baikal region to the intensification of the influence of the Indo-Asian collision. Unfortunately, the spatio-temporal framework of instrumental observations in the Baikal region limits the statistical investigation of the seismic moments of small and moderate shocks. Such investigations, if extended to the Mongolian-Siberian region, would yield qualitatively new information relating seismic moments of the earthquakes to the influence of global and regional processes, and be useful for the medium-term prediction of large earthquakes in the BSZ (Klyuchevskii and Demyanovich, 2002b).

Acknowledgements

I would like to thank V.M. Demyanovich for his assistance in preparing maps. I am also grateful to S. Gao, G. Ranalli and an anonymous reviewer for their help in the revision of preliminary versions of the manuscript.

References

- Brune, J.N., 1970. Tectonic stress and the spectra of seismic shear waves from earthquakes. *Journal of Geophysical Research* 75, 4997–5009.
- Dyadkov, P.G., Melnikova, V.I., Sankov, V.A., Nazarov, L.A., Nazarova, L.A., Timofeev, V.Yu., 2000. Recent dynamics of the Baikal rift: episode of compression followed by extension in 1992–1996. *Doklady Akademii Nauk* 372, 99–103. (in Russian).
- Gao, S., Davis, P.M., Liu, H., Slack, P.D., Zorin, Yu.A., Mordvinova, V.V., Kozhevnikov, V.M., Meyer, R.P., 1994. Seismic anisotropy and mantle flow beneath the Baikal rift zone. *Nature* 371, 149–151.
- Golenetsky, S.I., 1990. Problems of seismicity of the Baikal rift zone. *Journal of Geodynamics* 11, 293–307.
- Hough, S.E., Dreger, D.S., 1995. Source parameters of the 23 April 1992 M 6.1 Joshua Tree, California earthquake and its aftershocks: empirical Green's function analysis of GEOS and TERRASCOPE data. *Bulletin of Seismological Society of America* 85, 1576–1590.
- Klyuchevskii, A.V., 1998. Dynamic source parameters of Mongolian earthquakes. *Volcanology and seismology* 19, 377–387.
- Klyuchevskii, A.V., 2000. Spatio-temporal variations of seismic moments of earthquake sources in the Baikal region. *Doklady Akademii Nauk* 373, 681–683. (in Russian).
- Klyuchevskii, A.V., Demyanovich, V.M., 2002a. State of seismic strain of the Earth's crust in the Baikal region. *Doklady Akademii Nauk* 382, 816–820. (in Russian).
- Klyuchevskii, A.V. & Demyanovich, V.M., 2002b. Geodynamics and seismicity of the Baikal region (from the instrumental data of 1968–1994). In: *Proceedings of the 4th International Conference "Problems of Geocosmos"*, St Petersburg State University, pp. 311–315.
- Klyuchevskii, A.V., 2003. Specific features of the state of stress and strain of the Earth's crust in the Baikal region. *Doklady Akademii Nauk* 389, 398–403. (in Russian).
- Kopnischev, Yu.F., Spilker, G.L., 1980. Spatio-temporal characteristics of large earthquake sources of different faults. *Izvestia Akademii Nauk SSSR, Fizika Zemli* 9, 3–11. (in Russian).
- Logatchev, N.A., Zorin, Yu.A., 1987. Evidence and cause of the two-stage development of the Baikal rift. *Tectonophysics* 143, 225–234.
- Logatchev, N.A., Zorin, Yu.A., 1992. Baikal rift zone: structure and geodynamics. *Tectonophysics* 208, 273–286.
- Logatchev, N.A., 1993. History and geodynamics of the Lake Baikal rift in the context of the Eastern Siberia rift system: a review. *Bulletin des Centres de Recherches Exploration—Production Elf Aquitaine* 17, 2, 353–370.
- Molnar, P., Tapponnier, P., 1975. Cenozoic tectonics of Asia: Effects of continental collision. *Science* 189, 4201, 419–426.
- Petit, C., Deverchere, J., Houdry, F., Sankov, V.A., Melnikova, V.I., Delvaux, D., 1996. Present day stress field changes along Baikal rift and tectonic implications. *Tectonics* 15, 1171–1191.
- Rautian, T.G., 1964. On determination of energy of earthquakes at distances up to 3000 km. In: *Experimental seismics*. *Trudy Instituta Fiziki Zemli Akademii Nauk SSSR*, 32 (193), pp. 86–93 (in Russian).
- Solonenko, A.V., Solonenko, N.V., Melnikova, V.I., Steiman, E.A., 1996. The analysis of spatial-temporal structure of seismicity in the Baikal rift zone. In: Schenk, X. (Ed.), *Earthquake Hazard and Risk*. Kluwer Academic Publishers, The Netherlands, pp. 49–62.
- Solonenko, A.V., Solonenko, N.V., Melnikova, V.I., Shteiman, E.A., 1997. The seismicity and earthquake focal mechanisms of the Baikal rift zone. *Bulletin des Centres de Recherches Exploration—Production Elf Aquitaine* 21, 1, 207–231.
- Zoback, M.L., 1992a. First- and second-order patterns of stress in the lithosphere: The World Stress Map project. *Journal of Geophysical Research* 97, 11703–11728.
- Zoback, M.L., 1992b. Stress field constraints on intraplate seismicity in Eastern North America. *Journal of Geophysical Research* 97, 11761–11782.